Polymer Chemistry

PAPER

View Article Online
View Journal | View Issue

Cite this: *Polym. Chem.*, 2025, **16**, 696

# Supramolecular bottlebrush copolymers from crown-ether functionalized poly(*p*-phenylenevinylene)s†

Anahita Keer, Arielle Mann, Chengyuan Wang and Marcus Weck *

Received 31st October 2024,
Accepted 12th December 2024

DOI: 10.1039/d4py01225a

rsc.li/polymers

The discovery of living, chain-growth polymerizations of poly(*p*-phenylenevinylene)s (PPVs) allows for low dispersed, controlled, and architecturally complex PPV-based polymers. This contribution presents the synthesis of PPVs functionalized with crown-ethers on each repeat unit that assemble with chain-end functionalized monotelechelic poly(styrene)s (PS) containing a terminal amine salt to form pseudorotaxane-based bottlebrush copolymers. The PPVs are synthesized by living ring-opening metathesis polymerization (ROMP) and the PS through atom-transfer radical polymerization (ATRP). The bottlebrush copolymer formation was confirmed by nuclear magnetic resonance spectroscopy, gel-permeation chromatography, isothermal titration calorimetry, dynamic light-scattering, wide-angle X-ray scattering, and optical spectroscopy. This work depicts the first example of a backbone modified PPV synthesized through ROMP and introduces a versatile strategy towards supramolecular bottlebrush copolymers containing conducting polymers. Our methodology lends itself to supramolecular materials for applications in chemical sensing, optoelectronics, and fluorescent imaging.

## Introduction

Organic conducting polymers, such as poly(*p*-phenylenevinylene) (PPV), are π-conjugated polymers with desirable optical and electrical properties.[1] PPVs have been used in devices such as organic light-emitting diodes (OLEDs), organic photovoltaic cells (OPVs), and as fluorescent probes in biomedical applications.[2] Substituting PPVs with solubilizing side-chains, such as alkoxy groups, makes this rigid-rod polymer solution processable.[3]

The discovery of living chain-growth polymerization of cyclophanedienes to yield PPVs using ruthenium catalysts has unlocked the development of well-defined PPV-based materials, with tuneable properties (Scheme 1).[3,4] [2.2] *para*-cyclophanediene (*p*Cpd) is polymerized by ring-opening metathesis polymerization (ROMP) to yield PPVs in a living, chain-growth manner with control over molecular weights, dispersities, and end-group identities.[4,5] The living character of ROMP also allows for the formation of block copolymers.[6] Recently, the Weck group reported dealkylating *para*-substituted *p*Cpds with complex side-chains that can be polymerized.[7,8]

Macromolecular architecture impacts polymer properties, such as packing, glassy states, melt temperatures, crystallinity, viscosity, and optical activity.[9–12] Bottlebrush copolymers are composed of linear polymers emanating from a main-chain, whose identity and density impacts polymer properties.[13] Linear PPVs have been widely reported but more complex PPV architectures are rare and PPV-based bottlebrush copolymers have not been reported to date.[7,14,15]

Over the past decade, to gain control over macromolecular architecture, the Weck group used molecular recognition units (MRUs) featuring noncovalent interactions such as hydrogen bonding, metal coordination, or π–π stacking to directionally self-assemble polymers into complex 3D structures.[16–21] Macrocyclic crown-ethers are prominent MRUs that form host–guest complexes with a range of both inorganic and organic cations.[17,22,23] Combining hydrogen bonding, coulombic interactions, electrostatic forces, and size complementarity, crown-ethers can recognize specific alkali metals and ammonium salts, resulting in the formation of pseudorotaxanes.[24–26] We

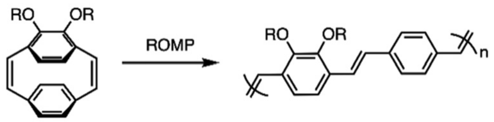

Scheme 1 Ring-opening metathesis polymerization (ROMP) of *ortho*-substituted-alkoxy-[2.2] *para*-cyclophanediene. R = alkyl side-chain.

---

Department of Chemistry and Molecular Design Institute, New York University, New York, NY 10003, USA. E-mail: marcus.weck@nyu.edu

† Electronic supplementary information (ESI) available. See DOI: https://doi.org/10.1039/d4py01225a

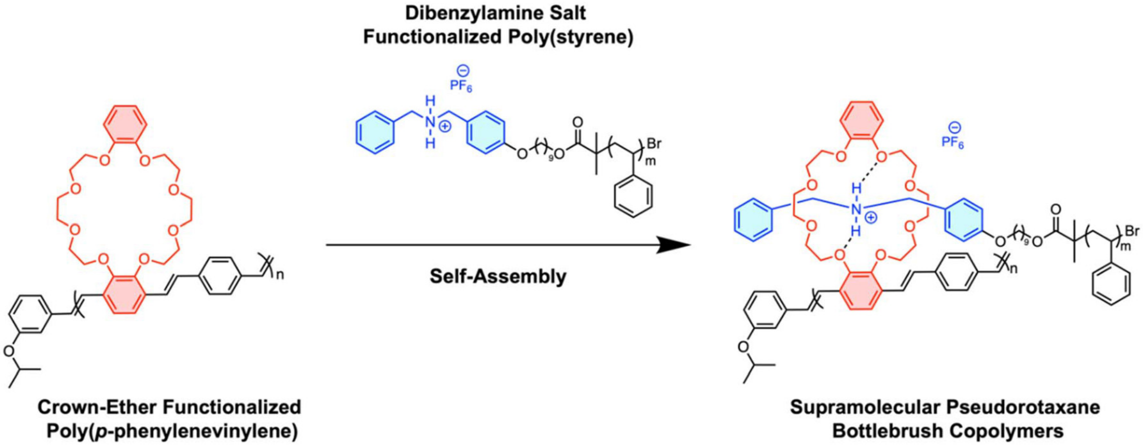

**Scheme 2** Synthesis of supramolecular bottlebrush copolymers based on host–guest interactions between crown-ether functionalized poly(*p*-phenylenevinylene) and dibenzyl amine end-functionalized poly(styrene).

rationalize that installing crown-ethers and ammonium salts on two separate polymers, one along each repeat unit of polymer A and the other at the terminus of polymer B, supramolecular bottlebrush copolymers can be constructed (Scheme 2).[18,27–29]

In this contribution, we report the realization of a PPV-based supramolecular bottlebrush copolymer (Scheme 2). Our design is based on *ortho*-substituted *p*Cpds appended with dibenzo-24-crown-8 (DB24C8) and polymerized *via* ROMP to afford crown-ether containing PPVs (CE-PPVs). Using atom-transfer radical polymerization (ATRP), poly(styrene) (PS) was functionalized with a complementary cationic dibenzyl ammonium ($DBA^+$) at one chain-end ($PS\text{-}DBA^+$).[30] Pseudorotaxane formation yielded supramolecular bottlebrushes which were characterized by nuclear magnetic resonance (NMR) spectroscopy, gel-permeation chromatography (GPC), isothermal titration calorimetry (ITC), dynamic light-scattering (DLS), wide-angle X-ray scattering (WAXS), and optical spectroscopy. Our work provides a platform to develop supramolecular functionalized materials for applications in areas such as sensing, optoelectronics, and fluorescent imaging.

## Results and discussion

### Synthesis

The *ortho*-substituted *p*Cpd, **9**, was synthesized in close analogy to our previous report, starting with catechol.[7]

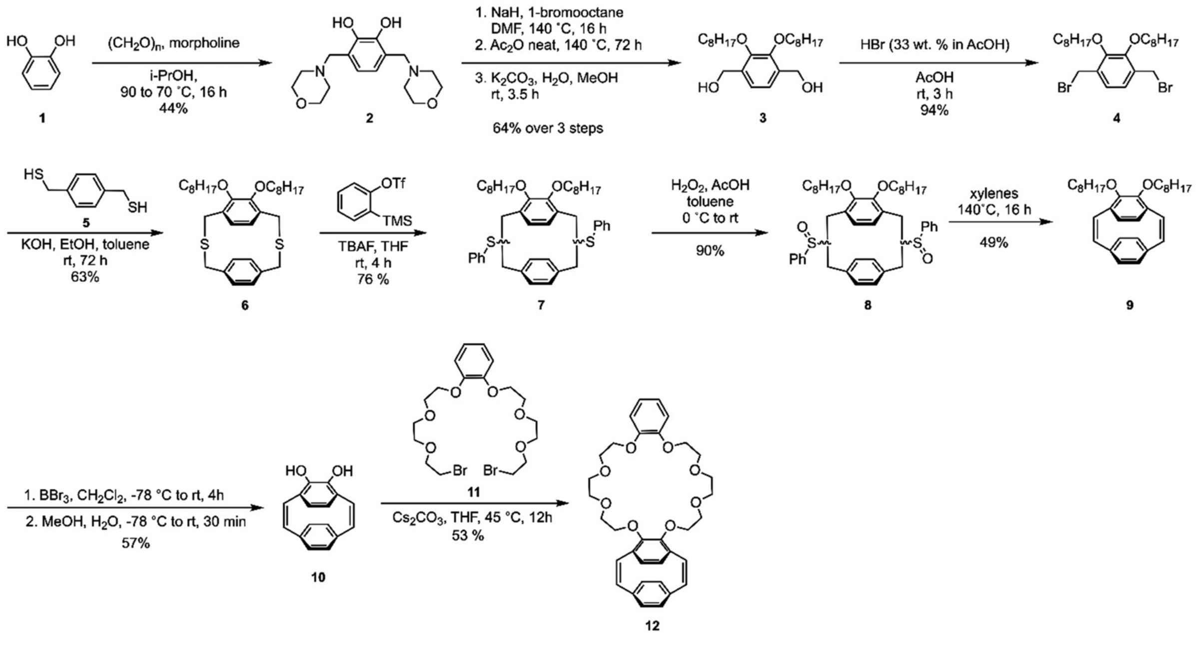

**Scheme 3** Synthetic route towards CE-*p*Cpd, **12**.

Morpholine groups were installed using a Mannich reaction. For solubility, alkoxy groups were appended and the Mannich base was exchanged over two steps to afford diol **3** which was converted to the dibromomethylated product, **4**. Under dilute conditions, **4** was reacted with **5** to form the [3.3] dithia-*para*-cyclophane **6**. Compound **6** underwent a benzyne-induced Stevens rearrangement to give compound **7**, which was oxidized to form compound **8**. The sulfoxides were thermally eliminated to contract the ring resulting in diene **9**. Compound **9** was treated with boron tribromide to generate the catechol-like *p*Cpd **10**. It should be noted that when *para*-substituted *p*Cpds undergo dealkylation, the dihydroxide oxidizes to form diquinones. The same was not observed with the *ortho*-substituted *p*Cpd.[31] Compound **10** was reacted with dibromide **11** under basic conditions to give the desired crown-ether *p*Cpd (CE-*p*Cpd) monomer **12** (Scheme 3).

We investigated the living nature of the ROMP of **12** (Scheme 4) using Hoveyda-Grubbs' second generation initiator (HGII) (Fig. 1). All resulting polymers showed low dispersities ($Đ$ < 1.33) with full monomer consumption (Fig. 1a). We observed a linear relationship for each of the monomer to initiator feed ratios ([M]/[I]) plotted with the molecular weights ($M_n$) (Fig. 1b) (**13a–d**). ROMP gives PPVs with a *cis–trans* conformation that can be photo-isomerized under UV-light to give the all-*trans*-CE-PPV, **14**. The absolute molecular weights were determined by $^1$H NMR spectroscopy by integrating the isopropoxy protons on the initiating end-group from HGII and comparing them to the methylene protons. The livingness of the polymerization was further elucidated by preparing a diblock copolymer, which supported the presence of an active chain-end (**15**) (ESI, Scheme S2†). Again, complete monomer consumption was observed by *in situ* $^1$H NMR spectroscopy and end-group identity by $^1$H NMR spectroscopy and MALDI-ToF-MS (ESI, Fig. S3†). These results show that the polymerization proceeded without chain-termination or chain-transfer and the resultant polymers had low dispersities with control over polymer properties, *i.e.*, **13** was polymerized in a living, chain-grown manner.[31,32]

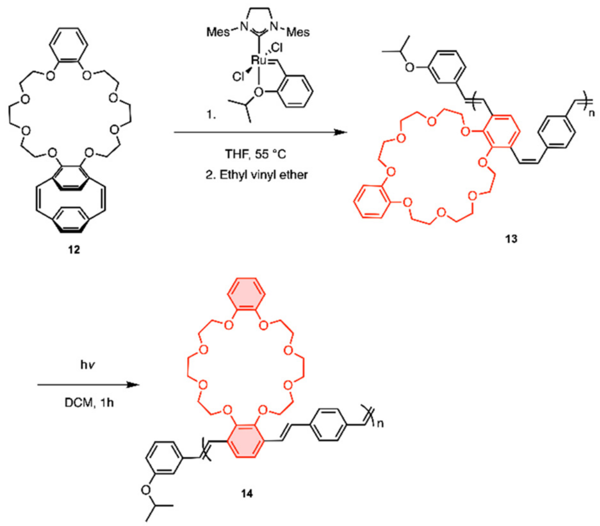

**Scheme 4** ROMP of CE-*p*Cpd, **12**, and photo-isomerization at 395 nm.

The optical properties of the PPV polymers were then investigated. Consistent with previous literature, as the molecular weight of the CE-PPVs increased, the absorbance maxima decreased while emission remained similar (Table 1).[33] Compared to *para*-substituted PPVs, the CE-PPV's blue-shifted absorbance and emission wavelength maxima are consistent with *ortho*-substitution of PPVs as reported in the literature.[7,33,34] Previously, the Weck group published the synthesis of *ortho–para*-substituted tetra-alkoxy PPVs.[7] These PPVs absorb at 416 nm and emit at 524 nm, whereas the CE-PPVs absorb at 353 nm and emit at 483 nm. The substituent identity and location differ between these two PPVs. The crown-ether substituent has a significant impact on the hypsochromic shift of both optical parameters. When the *cis–trans*-CE-PPV (**13b**) photo-isomerized to the all-*trans*-**14**, the absorbance red-shifted and emission remained the same, consistent with increasing conjugation length due to lower steric crowding around the *trans* vinylene bonds (ESI, Fig. S4 and S5†).[7]

The second required building block towards bottle brush copolymers is a polymer containing an amine end group (Scheme 5). Monotelechelic PS was polymerized using ATRP

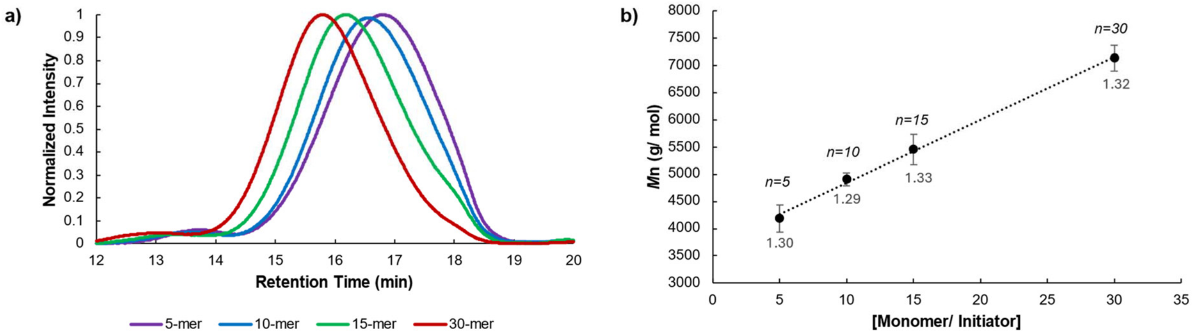

**Fig. 1** (a) Molecular weight distribution of polymers **13a–d** (GPC in THF). (b) Dependence of $M_n$ as measured by GPC of polymers **13a–d** on the [M]/[I] ratio. Here, **13a**, $n$ = 5, **13b**, $n$ = 10, **13c**, $n$ = 15, and **13d**, $n$ = 30. Dispersity values of the respective polymers are denoted in the plot.

Table 1 GPC data and optical characterization of CE-PPVs

| PPV | [M/I] | $M_{n,Calc.}$ [a] | $M_{n,\ GPC}$ [b] | $M_{n,\ NMR}$ [c] | $Đ$ | Yield % | Abs. $\lambda_{max}$ [d] | Em. $\lambda_{max}$ [d] |
|---|---|---|---|---|---|---|---|---|
| **13a** | 5 | 3035 | 4200 | 3035 | 1.30 | 97 | 361 | 481 |
| **13b** | 10 | 5809 | 4900 | 6483 | 1.29 | 96 | 353 | 483 |
| **13c** | 15 | 8783 | 5500 | 9357 | 1.33 | 85 | 349 | 481 |
| **13d** | 30[e] | 17 402 | 7150 | — | 1.32 | 83 | 347 | 482 |
| **14** | 10-*trans* | 5809 | 6400 | — | 1.40 | Quant. | 441 | 482 |
| **15** | Diblock[e] | 8164 | 29 400 | — | 1.26 | 87 | 408 | 516 |

[a] $M_n$ values were calculated based on the targeted degree of polymerization. [b] $M_n$ GPC values were determined against poly(styrene) standards. The mobile phase was THF and the detector was UV-Vis. [c] The crown-ether protons of the CE-PPV were integrated against the isopropoxy proton of the end-group. [d] Measurements were done in dilute solutions of chloroform. [e] Feed ratio was too large for integration of signals.

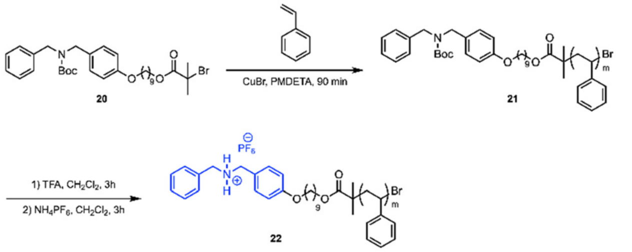

Scheme 5 Synthesis of telechelic PS-DBA$^+$, **22**.

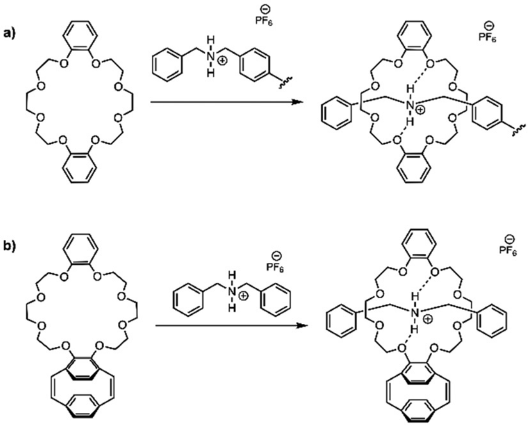

Scheme 6 Pseudorotaxane formation. (a) The host is commercially available DB24C8 and the guest is PS-DBA$^+$, **22**. (b) The host is CE-*p*Cpd, **12**, and the guest is commercially available DBA$^+$.

initiator **20** to yield polymer **21**.[21,30] The amine end-group was boc-protected during the polymerization due to the presence of an amine causing uncontrolled polymerization behavior.[17] Trifluoracetic acid was used to deprotect the amine and then hexafluorophosphate was added to install a non-coordinating counter-ion for the creation of the ammonium chain-end, **22**.

ATRP reached 40% conversion in four hours and was terminated to prevent any deviation from first-order kinetics.[35] Aliquots of the polymerization were taken every 30 minutes under an argon atmosphere. The $M_n$ of the aliquots, analyzed by GPC, increased with time to give monomodal polymers with narrow dispersities. The semilogarithmic plot showed that ATRP progressed with first-order kinetics, which indicates a living polymerization (ESI, Fig. S6†).

## Self-assembly

**Small molecule assemblies.** Dibenzo-24-crown-8 (DB24C8) and dibenzylammonium salt (DBA$^+$) are known to assemble spontaneously in aprotic solvents with an association constant ($K_a$) of $1.7 \times 10^3$ M$^{-1}$ in 1 : 1 chloroform/acetonitrile.[24] We first assembled commercially available DB24C8 and polymer **22**, PS-DBA$^+$ (Scheme 6a) and observed characteristic complexation using $^1$H NMR spectroscopy (ESI, Fig. S7†). Upon addition of excess PS-DBA$^+$, a new signal at $\delta$ = 4.10 ppm was observed that corresponds to "free" dibenzylammonium salt. Next, the ability of the small molecule host to form a pseudorotaxane was analyzed by complexing CE-*p*Cpd, compound **10**, with DBA$^+$ in a 1 to 1 ratio (Scheme 6b). The characteristic methylene peaks of the crown-ether appeared between $\delta$ = 3.52 and 4.16 ppm, and the benzylic peaks of the dibenzylamine salt appears at $\delta$ = 4.12 ppm. The complexed methylene peaks appeared at $\delta$ = 4.28, 4.63, and 4.94 ppm. The signal at $\delta$ = 4.08 ppm corresponds to the salt (ESI, Fig. S8†).

**Bottlebrush copolymer assembly.** After examining the small molecule assemblies, the self-assembly of the polymeric units was investigated (Scheme 7, and Fig. 2). The guest, PS-DBA$^+$ (**22**), was titrated into the host, CE-PPV (**13b**), to form the targeted polypseudorotaxane. The host–guest complex self-assembled in a 1 : 1 stoichiometric equivalence ratio (based on MRUs) in a solution of 1 : 1 chloroform and acetonitrile, chosen to fully solubilize the cationic salt. The complexed benzylic protons appeared at $\delta$ = 4.16 to 4.39 ppm and the complexed crown-ether protons appeared from $\delta$ = 3.28 to 3.42 ppm. New signals at $\delta$ = 2.78 and 2.55 ppm represent the uncomplexed and complexed acidic ammonium cation (Fig. 2).[36] Upon addition of excess triethylamine, the ammonium cation was deprotonated, and the crown-ether complexation dethreaded.[17] The complexed ammonium peaks disappeared and the benzylic protons of the dibenzyl amine appeared at $\delta$ = 3.68 ppm (ESI, Fig. S9†). The polymeric bottlebrush is, therefore, pH responsive.

Due to the overlapping and broad peaks of the polymers, association constant ($K_a$) was not successfully calculated through $^1$H NMR spectroscopy, so, isothermal titration calorimetry (ITC) using 1 : 1 $CHCl_3/CH_3CN$ as the solvent was per-

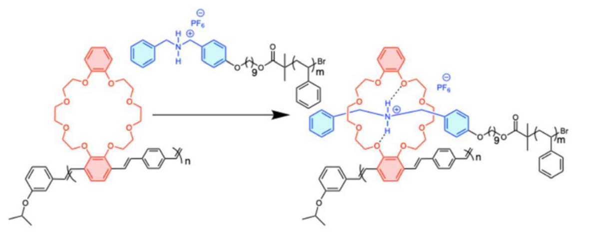

**Scheme 7** Bottlebrush copolymer assembly. The host is CE-PPV, **13b**, and the guest is PS-PBA$^+$, **22**.

formed. PS-DBA$^+$ (**22**) was titrated into CE-PPV (**13b**) and the heat of dilution of three blanks was subtracted from the measurement. The blanks were: solvent titrated into solvent, PS-DBA$^+$ titrated into solvent, and solvent titrated into CE-PPV. The host solution had a concentration of 0.105 mM and the guest solution of 0.085 mM. The $K_a$ was determined by a single-site binding model as $9.305 \times 10^4$ M$^{-1}$ ± 1.14 $10^4$ M$^{-1}$ and the stoichiometry ratio ($n$) was found to be 1.28 ± 0.09, which is similar to the 1 : 1 complexation seen in the small molecule counterparts (ESI, Fig. S10†). Please note that 10 equivalents of PS-DBA$^+$ (**22**) were titrated into 1 equivalent of CE-PPV (**13b**), based on having a 10-mer host polymer with 10 CE binding sites. The polymeric units associated a magnitude of order stronger than their small molecule counterparts ($1.7 \times 10^3$ M$^{-1}$).[24] We hypothesize that this is due to the increased π-stacking in the conjugated PPV system compared to the reported small molecule complexes.

The changes in the hydrodynamic radius ($R_h$) between CE-PPV (**13b**) and the assembled CE-PPV-PS-DBA$^+$ were characterized *via* dynamic light scattering (DLS) (Fig. 3a). The CE-PPV had an $R_h$ of 1.5 nm with a narrow size distribution, whereas the CE-PPV-PS-DBA$^+$ had a mean $R_h$ of 2.8 nm, with a wide size distribution. Since the pseudorotaxane was designed as a bottlebrush copolymer, there would be a high local concentration of tethered chains forced to extend away from the polymer backbone, resulting in a larger $R_h$ and wider size distribution. The assembly was analyzed by GPC, showing a decrease in elution time and an increase in dispersity (CE-PPV $Đ$ = 1.29, PS-DBA$^+$ $Đ$ = 1.04 and for CE-PPV-PS-DBA$^+$ $Đ$ = 1.36). This change in dispersity and retention time may indicate that a larger aggregate than the homopolymers was formed, which is most likely the bottlebrush copolymer (Fig. 3b).[21] It should be noted that the CE-PPV is a rigid-rod polymer while the PS-DBA$^+$ is coiled. The bottlebrush would have characteristics of both: a more coiled character than CE-PPV while being more rigid than the PS-DBA$^+$.

Optical data of the CE-PPV (**13b**), and the bottlebrush, CE-PPV-PS-DBA$^+$ were collected in 1 : 1 $CHCl_3/CH_3CN$ at a concentration of 0.46 μM. In this solvent mixture, compared to chloroform only, absorbance for the CE-PPV shifted from $\lambda_{max}$ = 353 to 362 nm, and the emission shifted from $\lambda_{max}$ = 482 to 506 nm.

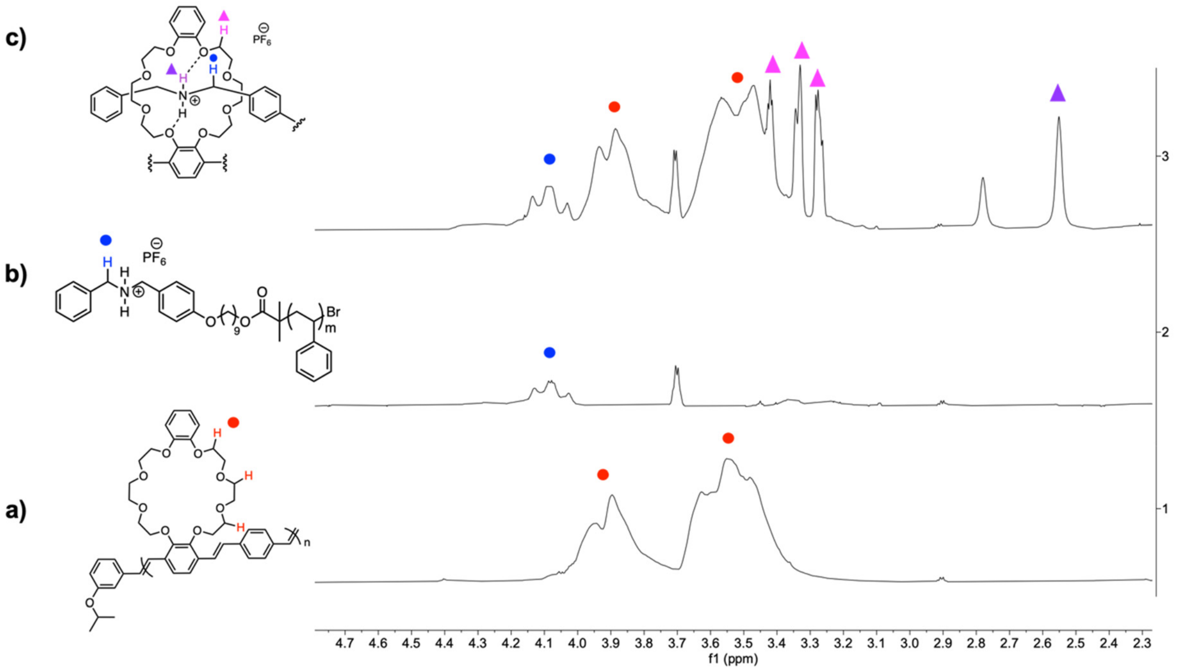

**Fig. 2** $^1H$ NMR spectral overlay of 1.00 mM CE-PPV (**13b**) with PS-DBA$^+$ (22) in 1 : 1 $CDCl_3/CD_3CN$ showing the supramolecular interaction resonances of the DBA$^+$ benzylic protons and CE protons. (a) Host–guest complex of CE-PPV and PS-DBA$^+$ in an equimolar ratio, (b) host PS-DBA$^+$ in 1 : 1 $CDCl_3/CD_3CN$, (c) guest CE-PPV in 1 : 1 $CDCl_3/CD_3CN$. The circles represent uncomplexed protons and the triangles represent complexed protons.

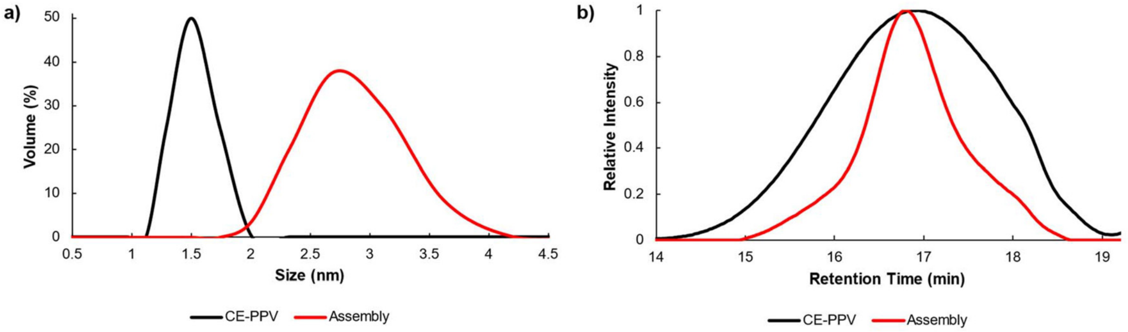

**Fig. 3** (a) DLS in 1 : 1 $CHCl_3/CH_3CN$ and (b) GPC characterization in THF, against linear PS standards, of homopolymer CE-PPV (**13b**) (black) and the supramolecular bottlebrush CE-PPV-PS-DBA$^+$ (red).

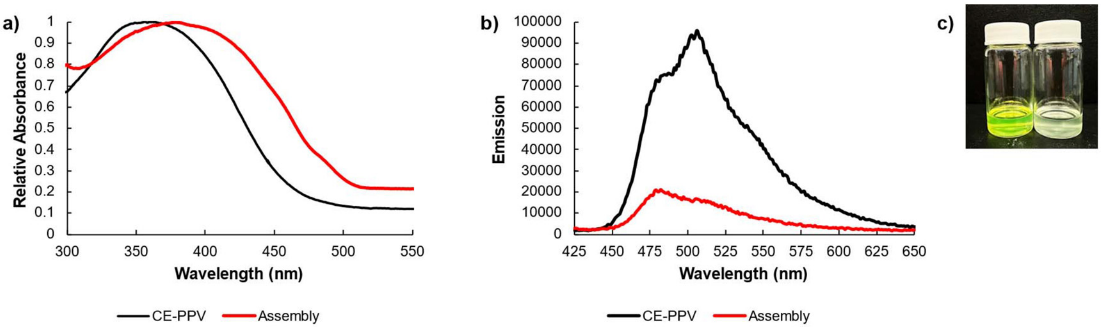

**Fig. 4** (a) Absorbance spectra and (b) emission spectra of homopolymer CE-PPV (**13b**) (black) and the supramolecular bottlebrush CE-PPV-PS-DBA$^+$ (red). (c) The CE-PPV has strong fluorescence (left) and the bottlebrush has quenched fluorescence (right).

Upon assembly, the absorbance red-shifted from $\lambda_{max}$ = 362 nm to 379 nm, which is similar to reported shifts in the literature for host–guest complexes (Fig. 4a). The emission shifted from $\lambda_{max}$ = 506 nm to 480 nm. The intensity saw a sharp, five-fold decrease in intensity from ~100 000 to 20 000, indicating that a guest was encapsulated into the host along the backbone (Fig. 4b). When a host–guest complex is formed in a conjugated system, the analyte (**22**) induced aggregation of the system elicits a quenching response (Fig. 4c).[37–40]

Wide-Angle X-Ray Scattering (WAXS) gave insights into the crystallinity and order of the assembled structure (Fig. 5). PPVs are known to have semi-crystalline domains that show a broad but strong scattering peak around $2\theta$ = 20°.[6] The CE-PPV (**13b**) spectra shows this signature peak from $2\theta$ = 18 to 21°. The Bragg's reflection at $2\theta$ = 22° corresponds to the intra-backbone repeat units, *i.e.*, the crown-ether substituent. The sharper peak could suggest that the crown-ether increases crystallinity of the CE-PPV as compared to unsubstituted or alkoxy-substituted PPVs. This may be because the crown-ether adds bulk and restricts the rotational freedom of the polymer. Features at $2\theta$ = 30, 31, and 37° ($d$ = 2.97, 2.88, and 2.43 Å) indicate $\pi$-stacking. The assembled unit does not display any short-range order features, but the peak at $2\theta$ = 9.5° corresponds to $d$ = 9.30 Å, indicating long-range order. The reflection at $2\theta$ = 5.5° was from Kapton, which held the samples during the experiment.

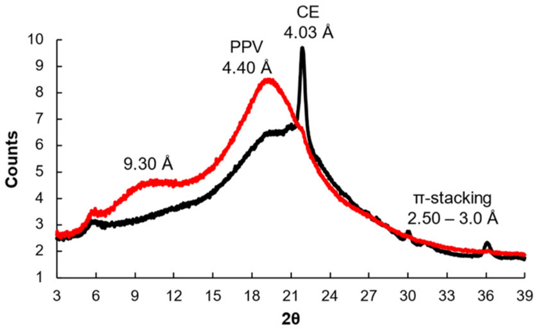

**Fig. 5** WAXS diffractograms corresponding to homopolymer CE-PPV (**13b**) (black) and the supramolecular bottlebrush CE-PPV-PS-DBA$^+$ (red).

## Conclusions

This contribution describes a highly strained CE-*p*Cpd which, after living ROMP, yields CE-PPVs with a high degree of control over polymer properties. The living character of the

ROMP was determined by $^1$H NMR spectroscopy, GPC, and with chain-extension experiments. The *cis–trans*-CE-PPVs were photo-isomerized to afford the conjugated all-*trans*-isomer. PS-DBA$^+$ was synthesized using ATRP with control over molecular weights and dispersities. Brush copolymers were formed *via* the host–guest driven assembly of CE-PPV and PS-DBA$^+$. The supramolecular bottlebrush is optically active, pH responsive, and semi-crystalline. This work depicts the first example of backbone-functionalized PPVs synthesized through ROMP and provides a platform to develop complex macromolecular architectures and supramolecular materials for applications in chemical sensing, optoelectronics, fluorescent imaging, and cross-linking.

## Data availability

The data supporting this article have been included as part of the ESI.†

## Conflicts of interest

There are no conflicts to declare.

## Acknowledgements

The authors acknowledge financial support from the National Science Foundation under award number CHE 2203929.

## References

1 A. J. Heeger, *Chem. Soc. Rev.*, 2010, **39**, 2354–2371.

2 A. J. Blayney, I. F. Perepichka, F. Wudl and D. F. Perepichka, *Isr. J. Chem.*, 2014, **54**, 674–688.

3 C. Y. Yu and M. L. Turner, *Angew. Chem., Int. Ed.*, 2006, **45**, 7797–7800.

4 A. Mann, M. D. Hannigan and M. Weck, *Macromol. Chem. Phys.*, 2023, **224**, 2200397.

5 N. Zaquen, L. Lutsen, D. Vanderzande and T. Junkers, *Polym. Chem.*, 2016, **7**, 1355–1367.

6 E. Elacqua, G. T. Geberth, D. A. Vanden Bout and M. Weck, *Chem. Sci.*, 2019, **10**, 2144–2152.

7 A. Mann and M. Weck, *ACS Macro Lett.*, 2022, **11**, 1055–1059.

8 C. Wang, A. Mann, M. D. Hannigan, R. H. Garvey, B. L. Dumlao and M. Weck, *Adv. Funct. Mater.*, 2024, **34**, 2313734.

9 G. Xie, M. R. Martinez, M. Olszewski, S. S. Sheiko and K. Matyjaszewski, *Biomacromolecules*, 2019, **20**, 27–54.

10 G. I. Peterson and T.-L. Choi, *Chem. Commun.*, 2021, **57**, 6465–6474.

11 E. Ahmed, C. T. Womble and M. Weck, *Macromolecules*, 2020, **53**, 9018–9025.

12 S. Catrouillet, L. Bouteiller, E. Nicol, T. Nicolai, S. Pensec, B. Jacquette, M. Le Bohec and O. Colombani, *Macromolecules*, 2015, **48**, 1364–1370.

13 S. T. Milner, *Science*, 1991, **251**, 905–914.

14 F. Menk, S. Shin, K.-O. Kim, M. Scherer, D. Gehrig, F. Laquai, T.-L. Choi and R. Zentel, *Macromolecules*, 2016, **49**, 2085–2095.

15 I. Cosemans, J. Vandenbergh, V. S. D. Voet, K. Loos, L. Lutsen, D. Vanderzande and T. Junkers, *Polymer*, 2013, **54**, 1298–1304.

16 R. Deng, C. Wang and M. Weck, *ACS Macro Lett.*, 2022, **11**, 336–341.

17 C. R. South, M. N. Higley, K. C. F. Leung, D. Lanari, A. Nelson, R. H. Grubbs, J. F. Stoddart and M. Weck, *Chem. – Eur. J.*, 2006, **12**, 3789–3797.

18 C. R. South, K. C. F. Leung, D. Lanari, J. F. Stoddart and M. Weck, *Macromolecules*, 2006, **39**, 3738–3744.

19 E. Elacqua, K. B. Manning, D. S. Lye, S. K. Pomarico, F. Morgia and M. Weck, *J. Am. Chem. Soc.*, 2017, **139**, 12240–12250.

20 S. K. Pomarico, D. S. Lye, E. Elacqua and M. Weck, *Polym. Chem.*, 2018, **9**, 5655–5659.

21 R. Deng, C. Wang, M. Milton, D. Tang, A. D. Hollingsworth and M. Weck, *Polym. Chem.*, 2021, **12**, 4916–4923.

22 L. Wang, L. Cheng, G. Li, K. Liu, Z. Zhang, P. Li, S. Dong, W. Yu, F. Huang and X. Yan, *J. Am. Chem. Soc.*, 2020, **142**, 2051–2058.

23 C. Zhang, K. Zhu, S. Li, J. Zhang, F. Wang, M. Liu, N. Li and F. Huang, *Tetrahedron Lett.*, 2008, **49**, 6917–6920.

24 P. R. Ashton, P. J. Campbell, P. T. Glink, D. Philp, N. Spencer, J. F. Stoddart, E. J. T. Chrystal, S. Menzer, D. J. Williams and P. A. Tasker, *Angew. Chem., Int. Ed. Engl.*, 1995, **34**, 1865–1869.

25 P. R. Ashton, I. Baxter, M. C. T. Fyfe, F. M. Raymo, N. Spencer, J. F. Stoddart, A. J. P. White and D. J. Williams, *J. Am. Chem. Soc.*, 1998, **120**, 2297–2307.

26 M. Xue, Y. Yang, X. Chi, X. Yan and F. Huang, *Chem. Rev.*, 2015, **115**, 7398–7501.

27 H. W. Gibson, M. A. Rouser and D. V. Schoonover, *Macromolecules*, 2022, **55**, 2271–2279.

28 L. He, X. Liu, J. Liang, Y. Cong, Z. Weng and W. Bu, *Chem. Commun.*, 2015, **51**, 7148–7151.

29 S.-J. Rao, Q. Zhang, J. Mei, X.-H. Ye, C. Gao, Q.-C. Wang, D.-H. Qu and H. Tian, *Chem. Sci.*, 2017, **8**, 6777–6783.

30 J.-S. Wang and K. Matyjaszewski, *J. Am. Chem. Soc.*, 1995, **117**, 5614–5615.

31 A. Mann, C. Wang, B. L. Dumlao and M. Weck, *ACS Macro Lett.*, 2024, **13**, 112–117.

32 R. B. Grubbs and R. H. Grubbs, *Macromolecules*, 2017, **50**, 6979–6997.

33 R. P. Quirk and B. Lee, *Polym. Int.*, 1992, **27**, 359–367.

34 Y. Janpatompong, A. M. Spring, V. Komanduri, R. U. Khan and M. L. Turner, *Macromolecules*, 2022, **55**, 10854–10864.

35 C.-Y. Yu and M. L. Turner, *Angew. Chem.*, 2006, **118**, 7961–7964.

36 A. Mohammad Rabea and S. Zhu, *Ind. Eng. Chem. Res.*, 2014, **53**, 3472–3477.

37 C. Wei, W. Yu, X. Liang, Y. Zhang, F. Zhang, W. Song, X. Ge, L. Wu and T. Xu, *J. Membr. Sci.*, 2022, **655**, 120580.

38 H. Liu, S. Wang, Y. Luo, W. Tang, G. Yu, L. Li, C. Chen, Y. Liu and F. Xi, *J. Mater. Chem.*, 2001, **11**, 3063–3067.

39 S. W. Thomas, G. D. Joly and T. M. Swager, *Chem. Rev.*, 2007, **107**, 1339–1386.

40 S. Wang, Y. Liu, H. Liu, G. Yu, Y. Xu, X. Zhan, F. Xi and D. Zhu, *J. Phys. Chem. B*, 2002, **106**, 10618–10621.